Precise Measurement of the Pion Axial Form Factor in the $\pi^+ \to e^+\nu\gamma$ Decay

E. Frlež,[1,*] D. Počanić,[1] V. A. Baranov,[3] W. Bertl,[2] M. Bychkov,[1] N. V. Khomutov,[3] A. S. Korenchenko,[3] S. M. Korenchenko,[3] T. Kozlowski,[4] N. P. Kravchuk,[3] N. A. Kuchinsky,[3] W. Li,[1] R. C. Minehart,[1] D. Mzhavia,[3] B. G. Ritchie,[6] S. Ritt,[2] A. M. Rozhdestvensky,[3] V. V. Sidorkin,[3] L. C. Smith,[1] I. Supek,[7] Z. Tsamalaidze,[5] B. A. VanDevender,[1] E. P. Velicheva,[3] Y. Wang,[1] H.-P. Wirtz,[2,†] and K. O. H. Ziock[1]

[1]*Department of Physics, University of Virginia, Charlottesville, VA 22904-4714, USA*
[2]*Paul Scherrer Institut, Villigen PSI, CH-5232, Switzerland*
[3]*Joint Institute for Nuclear Research, RU-141980 Dubna, Russia*
[4]*Institute for Nuclear Studies, PL-05-400 Swierk, Poland*
[5]*Institute for High Energy Physics, Tbilisi State University, GUS-380086 Tbilisi, Georgia*
[6]*Department of Physics and Astronomy, Arizona State University, Tempe, AZ 85287, USA*
[7]*Rudjer Bošković Institute, HR-10000 Zagreb, Croatia*

(Dated: 9 December 2003)

We have studied radiative pion decays $\pi^+ \to e^+\nu\gamma$ in three broad kinematic regions using the PIBETA detector and a stopped pion beam. Based on Dalitz distributions of 42,209 events we have evaluated absolute $\pi \to e\nu\gamma$ branching ratios in the three regions. Minimum χ^2 fits to the integral and differential (E_{e^+}, E_γ) distributions result in the axial-to-vector weak form factor ratio of $\gamma \equiv F_A/F_V = 0.443(15)$, or $F_A = 0.0115(4)$ with $F_V = 0.0259$. However, deviations from Standard Model predictions in the high-E_γ/low-E_{e^+} kinematic region indicate the need for further theoretical and experimental work.

PACS numbers: 11.30.Rd, 11.40.-q, 13.20.Cz, 14.40.Aq

In the Standard Model description of radiative pion decay $\pi^+ \to e^+\nu\gamma$, where γ is a real or virtual photon (e^+e^- pair), the decay amplitude M depends on the vector V and axial vector A weak hadronic currents [1]. Both currents contribute to the structure-dependent terms SD_V and SD_A associated with virtual hadronic states, while only the axial-vector current contributes to the inner bremsstrahlung process IB. Thus, it is convenient to write the decay amplitude as a sum: $M = M_{IB} + M_{SD}$. The IB amplitude is [2, 3]

$$M_{IB} = -\,i\frac{eG_FV_{ud}}{\sqrt{2}} f_\pi m_e \epsilon^{\mu *}\bar{e}\left(\frac{k_\mu}{kq} - \frac{p_\mu}{pq} + \frac{\sigma_{\mu\nu}q^\nu}{2kq}\right) \times (1-\gamma_5)\,\nu\,, \quad (1)$$

where p, k and q are the pion, electron and photon four-momenta, respectively, e and m_e are the electron charge and mass, G_F is the Fermi coupling constant, V_{ud} is the CKM quark mixing matrix element, while f_π is the pion decay constant.

The structure-dependent amplitude is parameterized by the vector and axial vector form factors, F_V and F_A:

$$M_{SD} = \frac{eG_FV_{ud}}{m_\pi\sqrt{2}}\epsilon^{\nu *}\bar{e}\gamma^\mu(1-\gamma_5)\nu \times [F_V\epsilon_{\mu\nu\sigma\tau}p^\sigma q^\tau + iF_A(g_{\mu\nu}pq - p_\nu q_\mu)]\,. \quad (2)$$

The conserved vector current (CVC) hypothesis [4, 5] relates F_V to the π^0 lifetime yielding $F_V = 0.0259(5)$ [6], which agrees with the relativistic quark model and chiral perturbation theory [7]. Chiral symmetry calculations [7, 8, 9] yield F_A in the range 0.010–0.014.

The combined $\pi \to e\nu\gamma$ event count of all previously published experiments is less than 1,200 events, while the overall uncertainties of the parameter $\gamma \equiv F_A/F_V$ extracted from data range from 12 % to 56 % [10, 11, 12, 13, 14, 15].

In this Letter we present a first analysis of the $\pi^+ \to e^+\nu\gamma$ ($\pi e2\gamma$) events recorded with the PIBETA detector in the course of a new measurement of the $\pi^+ \to \pi^0 e^+\nu$ ($\pi\beta$) branching ratio [16, 17] from 1999 to 2001.

The measurements were performed in the $\pi E1$ channel at the Paul Scherrer Institute (PSI), Villigen, Switzerland. The π^+ beam with $p \simeq 113$ MeV/c, $\Delta p/p \leq 1.3$ %, and 24 mr horizontal and vertical divergence, had an average intensity of $6.8 \cdot 10^5\,\pi^+$/s, and produced a $\sigma_{x,y} =$ 9 mm beam spot on target. A total of $2.2 \cdot 10^{13}$ π^+ stops were recorded during the running period.

The beam particles were first registered in a 3 mm thick beam counter (BC) placed ∼395 cm upstream of the detector center. The pions were slowed in a 30 mm thick active degrader (AD) and stopped in a 50 mm long segmented active target detector (AT) positioned in the center of the PIBETA detector. The BC, AD and AT detectors are all made of plastic scintillation material.

The e^+ and μ^+ beam contaminations determined by the time-of-flight method were small, 0.4 % and 0.2 %, respectively. The background from hadronic interactions was efficiently suppressed offline by cuts on the timing differences between the beam detectors and the CsI calorimeter.

The heart of the PIBETA detector is a spherical, 240-element, pure CsI electromagnetic calorimeter, 12 radiation lengths thick. The calorimeter achieves an rms energy resolution of $\sigma_E/E = 4.0$ % for π^0 mass reconstruction at rest, sub-ns timing resolution, and an angular

resolution of 2.0° for minimum ionizing particles (MIPs). Details of the detector design, construction, performance, along with other relevant information regarding our experimental method, are presented at the experiment Web site [18], and in Ref. [19].

Two sets of fast analog triggers accepted nearly all non-prompt pion decay events and a substantial fraction of muon decays, for energy depositions in the calorimeter exceeding a high threshold of HT $\simeq 51.7\,\mathrm{MeV}$, or a low threshold of LT $\simeq 4.5\,\mathrm{MeV}$. A pion stopping in the target initiates a 180 ns long pion gate πG, timed so as to sample pile-up events up to 30 ns prior to the π^+ stop pulse. Event triggers were generated on the basis of a coincidence of the πG gate, a beam anti-prompt veto, and a shower signal in the calorimeter.

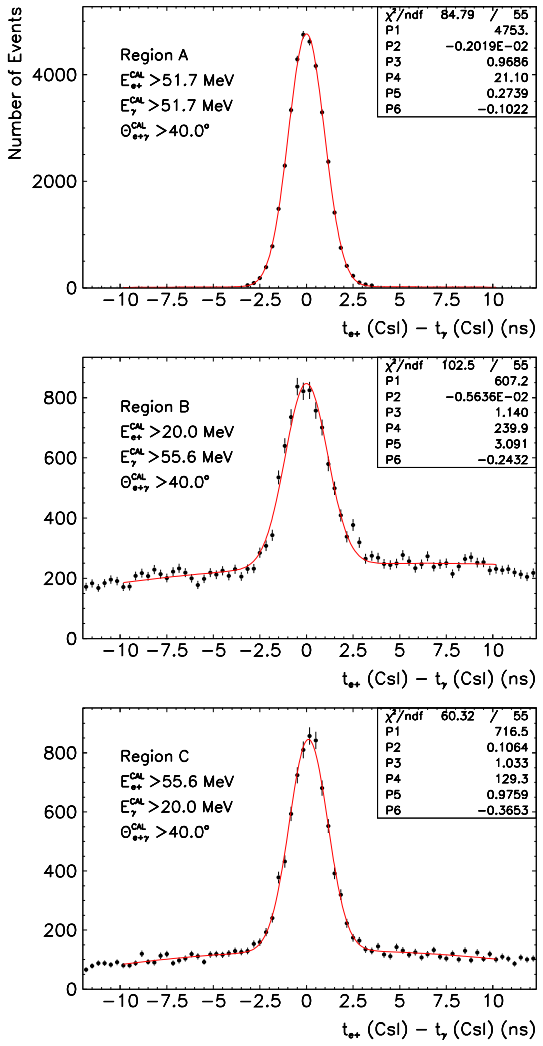

FIG. 1: The $\pi^+ \to e^+\nu\gamma$ class A events (the top panel) taken with two-arm calorimeter trigger are virtually background-free (save for the $\pi\beta$ contamination). The signal-to-background ratio for class B and class C events recorded with one-arm trigger is 3.8:1 and 7.6:1, respectively.

Charged particles emanating from the target were tracked by two cylindrical multi-wire proportional chambers [20] and a 20-piece thin plastic scintillator veto hodoscope (PV). The PV signals provided discrimination between the background protons and MIPs. MIP detection efficiencies were continuously monitored. The average efficiencies of the inner and outer MWPCs were $\epsilon_{C_1} = 93.7\%$ and $\epsilon_{C_2} = 97.9\%$, respectively. The average efficiency of the PV hodoscope was $\epsilon_{PV} = 98.9\%$. The overall inefficiency for distinguishing neutral and charged particles was therefore $1.5 \cdot 10^{-5}$.

$\pi \to e\nu\gamma$ candidate events were selected from the two-arm HT and prescaled one-arm HT data sets by requiring one neutral shower in the calorimeter in coincidence with a positron track. In cases where there was more than one possible coupling (i.e., more than one neutral or positron track), the pair most nearly coincident in time was chosen. Our data set covers three kinematic regions:

A: $E^{\mathrm{cal}}_{e^+}, E^{\mathrm{cal}}_{\gamma} > 51.7\,\mathrm{MeV}$ (two-arm HT),

B: $E^{\mathrm{cal}}_{e^+} > 20.0\,\mathrm{MeV}$, $E^{\mathrm{cal}}_{\gamma} > 55.6\,\mathrm{MeV}$ (one-arm HT),

C: $E^{\mathrm{cal}}_{e^+} > 55.6\,\mathrm{MeV}$, $E^{\mathrm{cal}}_{\gamma} > 20.0\,\mathrm{MeV}$ (one-arm HT),

where the superscript "cal" refers to values measured in the CsI calorimeter. In all three regions the relative angle $\theta^{\mathrm{cal}}_{e^+\gamma} > 40.0°$.

The signal-to-background ratios S/B are shown in Fig. 1 where the time differences between the radiative photon and the positron tracks are histogrammed. The high energy pairs of class A show virtually no background ($S/B \geq 300$), while the class B (C) events with lower energy positrons (photons) have $S/B = 3.8$ (7.6).

We define the coincidence time window by $\Delta t_{\mathrm{I}} \equiv |t_{e^+} - t_\gamma| \leq 5\,\mathrm{ns}$. The accidental background was sampled in two sidebands Δt_{O}, $-10\,\mathrm{ns} < t_{e^+} - t_\gamma < -5\,\mathrm{ns}$ and $5\,\mathrm{ns} < t_{e^+} - t_\gamma < 10\,\mathrm{ns}$.

The accidental background is dominated by positrons from $\pi \to e\nu$ or the π-μ-e decay chain, accompanied by an unrelated accidental neutral shower. This background was removed by subtracting histograms of observables projected using the out-of-time cut Δt_{O} from the in-time histograms projected via the Δt_{I} cut.

In addition to shower energies, we also measured the directions of the positron and photon, thus overdetermining the final three-body state. The positron direction was fixed using MWPC hits, while the photon direction was reconstructed from the pattern of hits in the calorimeter. Events with kinematics incompatible with the $\pi \to e\nu\gamma$ decay were rejected in the final data sample.

The time distributions of the $\pi \to e\nu\gamma$ events with respect to the π^+ stop time are plotted in Fig. 2. The fitted exponential curves are consistent with the π^+ lifetime and demonstrate the purity of the final data set.

Non-accidental background sources are (1) $\pi\beta$ events for which one π^0 decay photon converts in the target,

producing a charged track in the detector and (2) two-clump showers originating from a single $\pi \to e\nu$ positron when a secondary shower photon or positron interacts in the calorimeter far enough from the primary hit to appear as a separate clump ("split-clump" events).

Starting from the measured net yield of the $\pi\beta$ decay events, we have used the Monte Carlo (MC) simulation of γ conversions in the inner detector to determine that class (1) background events contribute 12.9 % of the signal in the kinematic region A and 4.3% (3.8 %) in region B (C). These $\pi\beta$ contaminations were subtracted in the calculation of $\pi \to e\nu\gamma$ yields. For the clump energy threshold $E^{\rm cal}_{e^+,\gamma} > 20.0\,$MeV used in the analysis the "split-clump" background (2) can be neglected.

We have normalized the radiative pion decay rate to the total branching ratio of the $\pi \to e\nu$ ($\pi e2$) events which were recorded in parallel using the prescaled one-arm calorimeter trigger. The energy spectrum of the $\pi^+ \to e^+\nu$ positrons is shown in Fig. 3. This procedure assures that most factors in the normalization, including the total number of decaying π^+'s and the combined tracking efficiency of e^+'s largely cancel out.

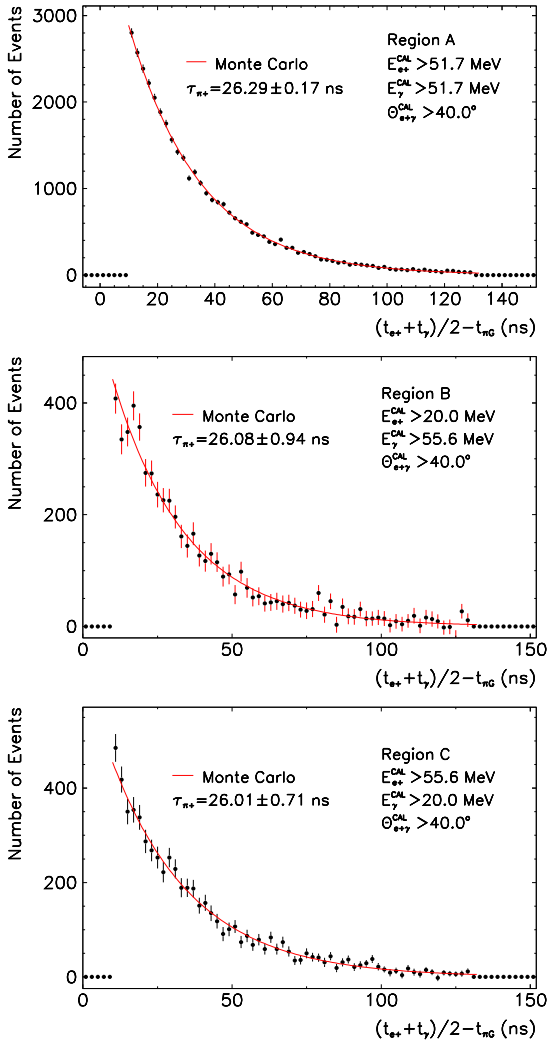

FIG. 2: $\pi^+ \to e^+\nu\gamma$ event timing spectra after subtraction of accidental background events. Predicted Monte Carlo decay functions are shown as full lines.

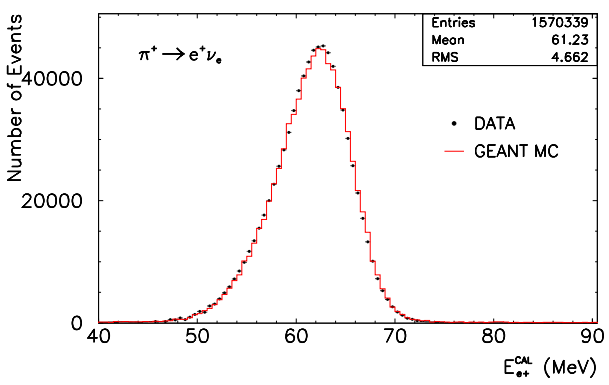

FIG. 3: Background-subtracted $\pi^+ \to e^+\nu$ energy spectrum taken with the one-arm trigger. The GEANT-simulated detector response is represented by the full line histogram.

The absolute branching ratio for the $\pi^+ \to e^+\nu\gamma$ decay can be calculated from the expression:

$$R_{\pi e2\gamma} = \frac{N_{\pi e2\gamma}\, p_{\pi e2\gamma}}{N_{\pi^+}\, g_\pi\, A_{\pi e2\gamma}\, \tau_l\, \epsilon_{\rm PV}\, \epsilon_{\rm C_1}\, \epsilon_{\rm C_2}}\,, \qquad (3)$$

where $N_{\pi e2\gamma}$ is the number of the detected $\pi \to e\nu\gamma$ events, $p_{\pi e2\gamma}$ is the corresponding prescaling factor (if any), N_{π^+} is the number of the decaying π^+s, $g_\pi = \int_{t_1}^{t_2} \exp(-t/\tau_{\pi^+})dt$ is the π^+ gate fraction, $A_{\pi e2\gamma}$ is the detector acceptance incorporating the appropriate cuts, and τ_l is the detector live time fraction. An analogous expression can be written for the total $R_{\pi e2}$ branching ratio. Combining the two, we obtain

$$R_{\pi e2\gamma} = R_{\pi e2}\frac{N_{\pi e2\gamma}\, p_{\pi e2\gamma}}{N_{\pi e2}\, p_{\pi e2}}\,\frac{A_{\pi e2}}{A_{\pi e2\gamma}}\,\frac{\epsilon_{\pi e2}}{\epsilon_{\pi e2\gamma}}\,, \qquad (4)$$

where the ϵ's denote the properly weighted products of $\epsilon_{\rm PV}\cdot\epsilon_{\rm C_1}\cdot\epsilon_{\rm C_2}$ for the two data sets. The detector acceptance ratio takes on values between 0.057 and 0.209, depending on the kinematic region.

The experimental acceptances depend on both the detector response and the decay amplitudes and are calculated in a Monte Carlo (MC) simulation. The GEANT [21] simulation of the PIBETA detector response included: (i) the detailed geometry of the active detectors and the passive support material, (ii) the measured detector energy and timing responses, (iii) event generators for π and μ decays including measured accidental pile-up rates, and (iv) the photo-absorption reactions in the CsI calorimeter incorporated in the GEANT code.

In the Standard Model the differential rate of the $\pi^+ \to$

$e^+\nu\gamma$ decay can be written in the form [1]:

$$\frac{d\Gamma_{\pi e2\gamma}}{dx\,dy} = \frac{\alpha}{2\pi}\Gamma_{\pi e2}\Big\{IB\,(x,y) + \left(\frac{F_V m_\pi^2}{2f_\pi m_e}\right)^2 \times \left[\,(1+\gamma)^2\,SD^+\,(x,y) + (1-\gamma)^2\,SD^-\,(x,y)\,\right] + \left(\frac{F_V m_\pi}{f_\pi}\right)\left[(1+\gamma)\,S^+_{\rm int}\,(x,y) + (1-\gamma)\,S^-_{\rm int}\,(x,y)\right]\Big\}, \quad (5)$$

where the IB, $SD^\pm$, and $S^\pm_{\rm int}$ (IB–SD interference) terms depend on the kinematic variables $x = 2E_\gamma/m_\pi$ and $y = 2E_e/m_\pi$; E_e and E_γ are the physical ("thrown") energies.

We took the PDG value $\Gamma(\pi e2)/\Gamma_{\rm total} = 1.230(4)\cdot 10^{-4}$ [6] and calculated the experimental branching ratios using the `MINUIT` least chi-square program [22]. We have added integral radiative corrections of $-1.0\,\%$ in region A, $-1.4\,\%$ in B, and $-3.3\,\%$ in C, to the theoretical $R_{\rm the}$'s [23]. The minimization program simultaneously fits two-dimensional $(E^{\rm cal}_{e^+}, E^{\rm cal}_\gamma)$ distributions in all three phase space regions, constraining the integrals to the experimental branching ratio values ($R_{\rm exp}$).

The acceptance $A_{\pi e2\gamma}$ is recalculated in every iteration step of our analysis with the cuts applied to the physical ("thrown") energies, E, following cuts applied to measured particle energies and angles, $E^{\rm cal}, \theta^{\rm cal}$. Hence, our experimental branching ratios can be compared directly with theoretical absolute decay rates.

The statistical uncertainties of the experimental yields are $0.6\,\%$, $1.7\,\%$ and $1.5\,\%$ for the regions A, B, and C, respectively. Systematic uncertainties of $1.8\,\%$ for region A, dominated by $\pi\beta$ background subtraction, $2.3\,\%$ and $3.1\,\%$ for regions B and C, respectively, both dominated by acceptance ratio uncertainties, were added in quadrature.

The dependence of the region-A experimental and theoretical branching ratio on the value of γ is shown in Fig. 4 (top), indicating two solutions. The positive γ solution is preferred by $\sim$ 50:1 once data from regions B and C are included in the analysis (bottom plot). We compare the experimental and theoretical branching ratios for the three phase space regions in Table I. We note that due to the large statistical and systematic uncertainties present in all older experiments, our values are consistent with previously published measurements. The best CVC fit to our data yields $\gamma = 0.443 \pm 0.015$, or $F_A = 0.0115(4)$ with $F_V \equiv 0.0259$. This result represents a fourfold improvement in precision over the previous world average, and is consistent with chiral Lagrangian calculations [7, 8, 9].

In summary, our experimental $\pi^+ \to e^+\nu\gamma$ branching ratios and energy distributions in kinematic regions A and C are compatible with the $(V-A)$ interaction. The sizable $19\,\%$ shortfall of the measured branching ratio compared to the theoretical one in region B dominates the total χ^2, and is disconcerting. Thus, in a fit restricted to region A data only, we obtain $\gamma = 0.480 \pm 0.016$, the same as when analyzing the combined data from regions A and C. Significantly, all previous studies save one (which, too, found an anomaly [15]), have analyzed only data with kinematics compatible with our region A.

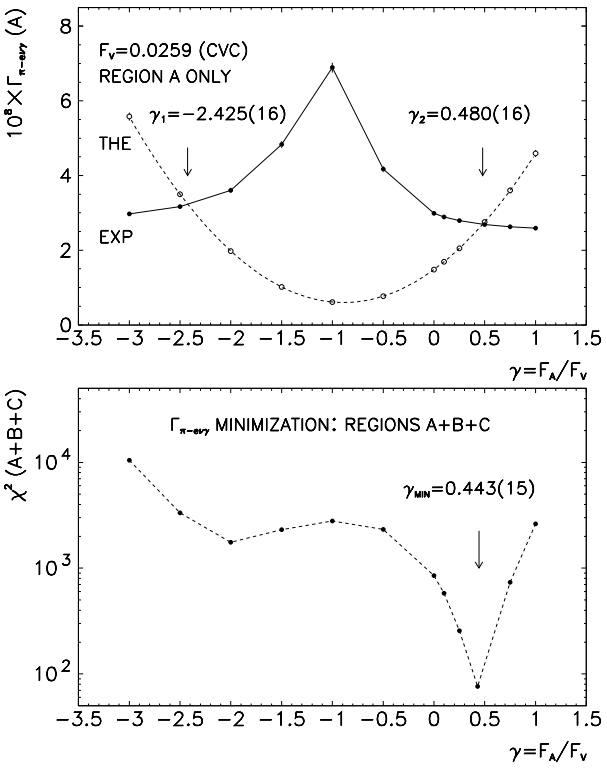

FIG. 4: Top: $\pi^+ \to e^+\nu\gamma$ branching ratio values as a function of $\gamma \equiv F_A/F_V$. The theoretical parabola follows from the $V-A$ model, Eq. (5). The experimental values reflect fits to region A data only. Bottom: minimum χ^2 values of simultaneous fits to the entire data set (regions A, B, C).

Taking the $(V-A)$ interaction and the CVC hypothesis as valid, the deficit could be caused by a specific detection or analysis inefficiency in our experiment, appearing dominantly in region B. Detailed cross-checks, including absolute total $\pi \to e\nu$, $\pi^+ \to \pi^0 e^+\nu$, $\mu \to e\nu\bar{\nu}$, as well as partial $\mu \to e\nu\bar{\nu}\gamma$ branching ratio evaluations from our data have thus far categorically excluded such inefficiencies [24]. Alternatively, the deficit could be caused by an inadequacy of the present $V-A$ description of the radiative pion decay, i.e., Eqs. (1), (2) and (5) along with the radiative corrections, or by an anomalous, non-$(V-A)$ interaction [15, 25, 26, 27]. We will focus on the region B discrepancy and the latter possibility in a separate forthcoming Letter, noting that our results clearly call for further theoretical and experimental work.

We thank W. A. Stephens, Z. Hochman, and the PSI experimental support group for invaluable help in preparing and running the experiment. We thank M. V. Chizhov and A. A. Poblaguev for fruitful dis-

TABLE I: Best-fit $\pi \to e\nu\gamma$ branching ratios obtained with $F_V = 0.0259$ (fixed) and $F_V = 0.0115(4)$ (fit); χ^2/d.o.f. = 25.4. Measured ($R_{\rm exp}$) and theoretical ($R_{\rm the}$) branching ratios are shown for the three indicated phase space regions. Radiative corrections are included in the calculations.

$E_{e^+}^{\rm min}$ (MeV)	$E_{\gamma}^{\rm min}$ (MeV)	$\theta_{e\gamma}^{\rm min}$	$R_{\rm exp}$ ($\times 10^{-8}$)	$R_{\rm the}$ ($\times 10^{-8}$)
50	50	–	2.71(5)	2.583(1)
10	50	40°	11.6(3)	14.34(1)
50	10	40°	39.1(13)	37.83(1)

cussions and comments, as well as E. A. Kuraev and Yu. M. Bystritsky for communicating to us their radiative correction results prior to publication. The PIBETA experiment has been supported by the U.S. National Science Foundation, the U.S. Department of Energy, the Paul Scherrer Institute, and the Russian Foundation for Basic Research.

* Corresponding author: frlez@virginia.edu
† Presently at: Philips Semiconductors AG, CH-8045 Zürich, Switzerland

[1] D. A. Bryman, P. Depommier, and C. Leroy, Phys. Rep. **88**, 151 (1982).
[2] S. M. Berman, Phys. Rev. Lett. **1**, 468 (1958).
[3] T. Kinoshita, Phys. Rev. Lett. **2**, 477 (1959).
[4] S. S. Gershtein and I. B. Zel'dovich, Zh. Eksp. Teor. Fiz. **29**, 698 (1955), [Soviet Phys.-JETP **2**, 576 (1956)].
[5] R. P. Feynman and M. Gell-Mann, Phys. Rev. **109**, 193 (1958).
[6] K. Hagiwara et al., Phys. Rev. D **66**, 010001 (2002).
[7] C. Q. Geng, I.-L. Ho, and T. H. Wu (2003), hep-ph/0306165.
[8] B. R. Holstein, Phys. Rev. D **33**, 3316 (1986).
[9] J. Bijnens and P. Talavera, Nucl. Phys. B **489**, 387 (1997).
[10] P. Depommier et al., Phys. Lett. **7**, 285 (1963).
[11] A. Stetz et al., Nucl. Phys. B **138**, 285 (1978).
[12] A. Bay et al., Phys. Lett. B **174**, 445 (1986).
[13] L. E. Piilonen et al., Phys. Rev. Lett. **57**, 1402 (1986).
[14] C. A. Dominguez and J. Solc, Phys. Lett. B **208**, 131 (1988).
[15] V. N. Bolotov et al., Phys. Lett. B **243**, 308 (1990).
[16] D. Počanić et al., *PSI R-89.01 Experiment Proposal*, Paul Scherrer Institute, Villigen (1992).
[17] D. Počanić et al. (2003), hep-ex/0312030.
[18] http://pibeta.phys.virginia.edu/.
[19] E. Frlež et al. (2003), hep-ex/0312017.
[20] V. V. Karpukhin et al., Nucl. Instrum. & Methods A **418**, 306 (1998).
[21] R. Brun et al., *GEANT 3.21*, CERN, Geneva (1994).
[22] F. James and M. Roos, *MINUIT—Function Minimization and Error Analysis*, CERN, Geneva (1989).
[23] E. A. Kuraev and Y. M. Bystritsky (2003), hep-ph/0310275.
[24] E. Frlež et al. (2003), hep-ex/0312025.
[25] P. Herczeg, Phys. Rev. D **49**, 247 (1994).
[26] A. V. Chernyshev et al., Mod. Phys. Lett. A **12**, 1669 (1997).
[27] M. V. Chizhov, Mod. Phys. Lett. A **8**, 2753 (1993).